Molecular Neurobiology (2021) 58:408–423
https://doi.org/10.1007/s12035-020-02115-w

ORIGINAL ARTICLE

Uric Acid Neuroprotection Associated to IL-6/STAT3 Signaling Pathway Activation in Rat Ischemic Stroke

Alicia Aliena-Valero[1,2] · Sergio Rius-Pérez[2] · Júlia Baixauli-Martín[2] · Germán Torregrosa[1] · Ángel Chamorro[3,4,5] · Salvador Pérez[2] · Juan B. Salom[1,2]

Received: 29 February 2020 / Accepted: 2 September 2020 / Published online: 22 September 2020

Abstract

Despite the promising neuroprotective effects of uric acid (UA) in acute ischemic stroke, the seemingly pleiotropic underlying mechanisms are not completely understood. Recent evidence points to transcription factors as UA targets. To gain insight into the UA mechanism of action, we investigated its effects on pertinent biomarkers for the most relevant features of ischemic stroke pathophysiology: (1) oxidative stress (antioxidant enzyme mRNAs and MDA), (2) neuroinflammation (cytokine and *Socs3* mRNAs, STAT3, NF-κB p65, and reactive microglia), (3) brain swelling (*Vegfa*, *Mmp9*, and *Timp1* mRNAs), and (4) apoptotic cell death (Bcl-2, Bax, caspase-3, and TUNEL-positive cells). Adult male Wistar rats underwent intraluminal filament transient middle cerebral artery occlusion (tMCAO) and received UA (16 mg/kg) or vehicle (Locke's buffer) i.v. at 20 min reperfusion. The outcome measures were neurofunctional deficit, infarct, and edema. UA treatment reduced cortical infarct and brain edema, as well as neurofunctional impairment. In brain cortex, increased UA: (1) reduced tMCAO-induced increases in *Vegfa* and *Mmp9/Timp1* ratio expressions; (2) induced *Sod2* and *Cat* expressions and reduced MDA levels; (3) induced *Il6* expression, upregulated STAT3 and NF-κB p65 phosphorylation, induced *Socs3* expression, and inhibited microglia activation; and (4) ameliorated the Bax/Bcl-2 ratio and induced a reduction in caspase-3 cleavage as well as in TUNEL-positive cell counts. In conclusion, the mechanism for morphological and functional neuroprotection by UA in ischemic stroke is multifaceted, since it is associated to activation of the IL-6/STAT3 pathway, attenuation of edematogenic VEGF-A/MMP-9 signaling, and modulation of relevant mediators of oxidative stress, neuroinflammation, and apoptotic cell death.

Keywords Ischemic stroke · Uric acid · Neuroprotection · IL-6/STAT3 pathway · Rat model

Alicia Aliena-Valero and Sergio Rius-Pérez contributed equally to this work.

✉ Salvador Pérez
salvador.perez-garrido@uv.es

✉ Juan B. Salom
salom_jba@gva.es

[1] Unidad Mixta de Investigación Cerebrovascular, Instituto de Investigación Sanitaria La Fe - Universitat de València, Torre A, Lab 5.05, Ave Fernando Abril Martorell 106, 46026 Valencia, Spain

[2] Departamento de Fisiología, Facultad de Farmacia, Universitat de València, Ave Vicent Andrés Estellés s/n, Burjassot, 46100 Valencia, Spain

[3] Institut d'Investigacions Biomèdiques August Pi i Sunyer (IDIBAPS), Barcelona, Spain

[4] Comprehensive Stroke Center, Department of Neuroscience, Hospital Clinic, Institut d'Investigacions Biomèdiques August Pi i Sunyer (IDIBAPS), Barcelona, Spain

[5] Departamento de Medicina, Universitat de Barcelona, Barcelona, Spain

Introduction

Uric acid (UA) is the end product of purine metabolism in humans and a major endogenous antioxidant in blood [1]. Moreover, systemic infusion of high UA doses was safe and increased serum antioxidant capacity in healthy humans [2]. As to acute ischemic stroke, the potential neuroprotective role of UA has been investigated in both preclinical and clinical scenarios. With regard to preclinical studies, mice heterozygous for a disrupted urate oxidase transgene (UOX+/−), with elevated serum UA levels, showed reduced brain damage and improved functional outcome after ischemic stroke [3]. Moreover, several studies have shown the neuroprotective effects of exogenous UA in murine models of acute ischemic stroke [4–10]; provided suitable doses are used [11].

In the clinical arena, a number of studies lend also support to the neuroprotective effect of UA in ischemic stroke patients. Serum UA level at stroke onset is a predictor biomarker of better prognosis, thus pointing to a protective effect on neurological outcome [12], confirmed by systematic reviews with meta-

analyses [13, 14]. From an interventional perspective, a pilot study showed that the administration of UA was safe, decreased oxidative stress markers, and prevented an early fall of serum UA in stroke patients treated with recombinant tissue plasminogen activator (rt-PA) [15, 16]. The moderately sized Efficacy Study of Combined Treatment With Uric Acid and rtPA in Acute Ischemic Stroke (URICO-ICTUS) trial [17] showed that the addition of UA to thrombolytic therapy resulted in a 6% absolute increase in the rate of excellent outcome at 90 days compared with placebo, with no safety concerns [18], and decreased the risk of early ischemic worsening [19]. Moreover, prespecified subgroup analyses showed significant benefits [20–23].

Despite the promising neuroprotective effects of UA in ischemic stroke, the mechanisms underlying UA benefits seem pleiotropic and are not completely understood. Beyond UA antioxidant effects, recent evidence points to transcription factors as UA targets for neuroprotection and vasculoprotection in acute ischemic stroke rodent models [24]. UA conferred neuroprotection against transient focal cerebral ischemia-induced oxidative stress via Nrf2/HO-1 pathway activation as well as BDNF and NGF expression upregulations [25]. On the other hand, UA treatment after stroke modulated the Krüppel-like factor 2/VEGF-A axis to protect endothelial cell functions and thus reduce brain damage [26]. In humans, endogenous serum UA levels positively associated with IL-6 [27], and exogenous UA administration further increased IL-6 levels [28]. Interestingly, IL-6 played a neuroprotective role through the activation of STAT3 transcription factor in mice subjected to ischemic stroke [29, 30], thus setting out the rationale for the hypothesis that IL-6/STAT3 signaling pathway is involved in the neuroprotective effects of UA in ischemic stroke.

The main objective of the present study was to gain insight into the pleiotropic role of UA in acute ischemic stroke through IL-6/STAT3 signaling pathway, using a rat model of transient focal cerebral ischemia. For this purpose, we investigated the effects of UA administration on pertinent biomarkers for the most relevant features of ischemic stroke pathophysiology: (1) oxidative stress (*Sod1*, *Sod2*, and *Cat* gene expression and malondialdehyde); (2) neuroinflammation (*Il6*, *Tnfa*, *Il1b*, and *Socs3* gene expression, STAT3, NF-κB p65, and reactive microglia); (3) brain swelling (*Vegfa*, *Mmp9*, and *Timp*1 gene expression); and (4) apoptosis (Bcl-2, Bax, caspase-3, and TUNEL-positive cells). Neurofunctional deficit, infarct, and edema were measured as the main outcomes to assess the neuroprotective effects of UA treatment.

Methods

Animals and Ethical Issues

A total of 40 male 12-week-old Wistar rats (300–350 g) from Charles River (Barcelona, Spain), housed under standard conditions with food and water ad libitum, were used in the study. Experiments were conducted in compliance with the legislation on protection of animals used for scientific purposes in Spain (RD 53/2013) and the EU (Directive 2010/63/EU). Protocols were approved by the Animal Experimentation Ethics Committee from IIS La Fe. The study was designed and conducted according to the STAIR/RIGOR guidelines [31, 32] regarding physiological monitoring, simple randomization, predefined exclusion criteria, allocation concealment, blinded assessment of several outcomes at different endpoints, and conflict of interest statement. The experimental timeline is summarized in Fig. 1.

Transient Focal Cerebral Ischemia

Animals were anesthetized by intraperitoneal injection of 5 mg/kg diazepam, 100 mg/kg ketamine, and 0.3 mg/kg atropine. Inhalatory anesthesia was maintained with 0.5–1% sevoflurane in 80% medicinal air plus 20% O_2. Transient right middle cerebral artery occlusion (tMCAO, 60 min) was performed by following the intraluminal suture procedure as originally described [33] and adapted to our experimental setup [34]. The procedure included continuous monitoring of cerebrocortical laser-Doppler flow (cortical perfusion, CP), arterial blood pressure and core temperature, and discontinuous measurement of blood glucose at preischemia (basal), ischemia, and reperfusion stages. Buprenorphine (s.c., 0.05 mg/kg) was used to provide analgesia. Six or 24 h after the ischemic insult, the animals were euthanized by intracardiac injection of KCl (200 mg/kg) under anesthesia to obtain the brain according to specific requirements for each determination.

Experimental Groups, Treatments, and Exclusion Criteria

Animals were randomly assigned to two experimental tMCAO groups: vehicle-treated and uric acid (UA)-treated rats. UA (Sigma-Aldrich, Madrid, Spain) was dissolved in Locke's buffer (vehicle, pH 7.2) and injected through the femoral vein (16 mg/kg) 20 min after the end of tMCAO. This dose was chosen based upon previous studies showing a neuroprotective effect of UA in murine models of ischemic stroke [5–11, 25]. UA concentrations in plasma (basal, 2, 4, and 6 h) and in homogenized cerebrocortical samples (6 h) were determined by spectrophotometry using commercial Uric acid-LQ kit (Ref. 41,000, Spinreact, Girona, Spain). Fourteen rats were excluded from the study according to predefined criteria, as detailed in Table 1.

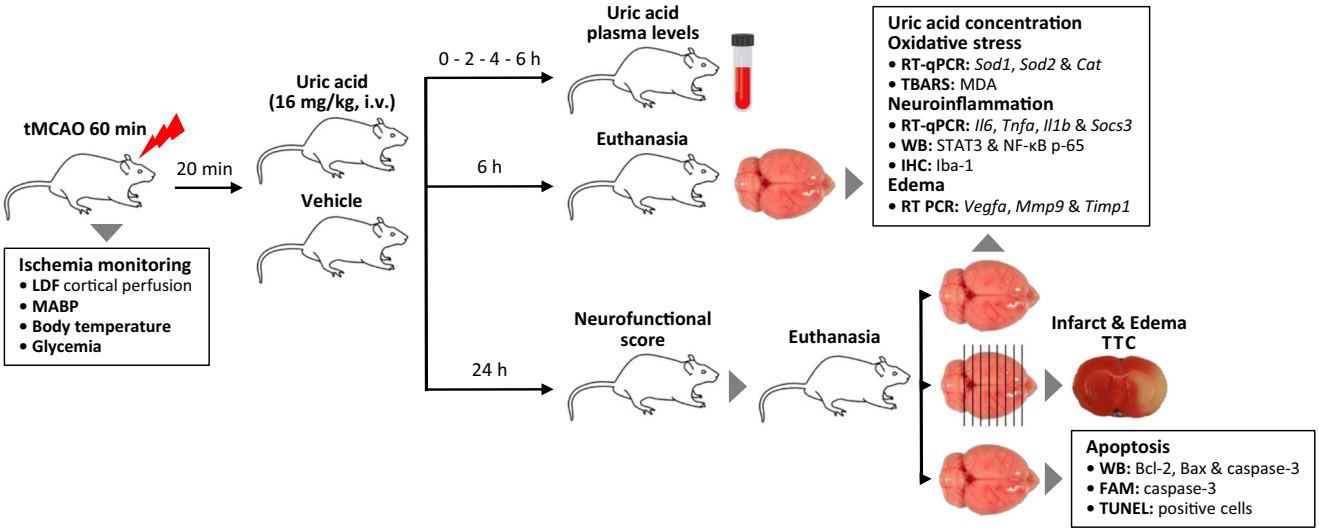

Fig. 1 Experimental timeline. Adult male Wistar rats underwent transient right middle cerebral artery occlusion (tMCAO, 60 min) by following the intraluminal suture procedure. The procedure included continuous monitoring of cerebrocortical laser-Doppler perfusion, mean arterial blood pressure (MABP) and core temperature, and discontinuous measurement of blood glucose at preischemia, ischemia, and reperfusion stages. Animals were randomly assigned to two experimental groups: vehicle-treated and uric acid (UA)–treated rats. UA was dissolved in vehicle and injected through the femoral vein (16 mg/kg) 20 min after the end of tMCAO. Plasmatic UA concentration (basal, 2, 4, and 6 h) was determined by spectrophotometry. Six or 24 h after the ischemic insult, the animals were euthanized to obtain the brain according to specific requirements for each determination. Neurofunctional deficit, infarct, and edema were the stroke outcome measures. Infarct volume, with edema correction, was assessed in 2-mm-thick coronal sections stained with 2,3,5-triphenyltetrazolium chloride (TTC). We investigated the effects of UA administration on cerebrocortical UA concentration and biomarkers for relevant features of ischemic stroke pathophysiology: oxidative stress, neuroinflammation, brain swelling, and apoptosis

Neurofunctional Evaluation and Measurement of Infarct and Edema Volumes

Twenty-four hours after the ischemic insult, rats were subjected to neurofunctional evaluation before euthanization as reported [9]. The severity of functional deficits was scored with four tests assessing: **a** spontaneous activity (moving/exploring = 0, no moving or moving only when pushed = 1); **b** circling to the left (none = 0, circling when elevated by the tail and pushed = 1, circling without displacement, spinning = 2; **c** parachute reflex: protective abduction of forelimbs (symmetrical = 0, asymmetrical, contralateral forelimb retracted = 1); and **d** resistance to left forepaw stretching (not allowed = 0, allowed = 1). The total score could range from 0 (no neurological deficits) to 5 (highest neurological deficits) or 6 (death).

Table 1 Animals excluded from the study according to predefined criteria

Criterion	Vehicle	Uric acid
No ischemia	0	1
No reperfusion	2	1
SAH	0	1
Dead before 12 h	2	3
No infarct	1	3

No ischemia: cortical perfusion (CP), monitored by laser-Doppler flowmetry, did not drop after filament insertion

No reperfusion: CP did not recover at all after filament withdrawal

SAH: subarachnoid hemorrhage

No infarct: in spite of a right ischemia-reperfusion pattern

Brain infarct volume was determined by the 2,3,5-triphenyltetrazolium chloride (TTC, Sigma-Aldrich) vital staining method [35], followed by morphometric analysis [34]. Briefly, rats were euthanized and the brain was sliced in seven 2-mm-thick coronal sections, which were immersed in a 2% solution of TTC in saline solution at 37 °C for 10 min, fixed in 10% phosphate-buffered formalin (pH 7.4) overnight, and digitally photographed for image analysis. Infarct volume was calculated with edema correction [34], separately for cortical and subcortical regions. The subtraction between raw and corrected infarcted hemisphere equals to the edema volume.

RT-qPCR Analysis of Gene Expression

Rats were euthanized, and a 2-mm-thick brain coronal section (0.2 to − 1.8 mm from bregma) was obtained. Ipsilateral (ischemic) and contralateral (non-ischemic) cortices were dissected, flash-frozen in liquid N_2, lyophilized, and grinded to obtain brain powder as reported [36]. For extraction of total RNA, brain powder samples were homogenized (T8.01 Ultra-Turrax, Ika, Staufen, Germany) in TRIzol reagent, centrifuged at 12,000×*g* for 10 min, the supernatant collected and mixed with chloroform, and centrifuged again. The upper aqueous

phase was mixed with isopropanol for RNA precipitation. The isolated RNA (2 μg/lane) was size-fractionated by electrophoresis in a 1% agarose/formalin gel and stained with ethidium bromide to assess RNA quality. RNA concentration was measured in a NanoDrop Lite spectrophotometer (Thermo Scientific, Waltham, MA, USA), and purity was determined by the OD 260/280 ratio.

The cDNA used as template for amplification in the qPCR assay was obtained by the reverse transcription reaction using PrimeScript RT reagent Kit (TaKaRa Bio, Kusatsu, Japan) according to the manufacturer's protocol, starting with equal amounts of RNA. The RNA level of the genes was analyzed by dsDNA binding dye SYBR Green PCR Master mix in an iQTM5 Multicolor Real-Time PCR Detection System (Bio-Rad, Hercules, CA, USA). Each reaction was run in triplicate, and the melting curves were constructed using Dissociation Curves Software (Bio-Rad) to ensure that only a single product was amplified. The specific primers used are shown in Table 2. The threshold cycle (CT) was determined, and the relative gene expression was expressed as follows: fold change = $2^{-\Delta(\Delta CT)}$, where $\Delta CT = CT_{target} - CT_{housekeeping}$, and $\Delta(\Delta CT) = \Delta CT_{treated} - \Delta CT_{control}$. *Actb* was used as housekeeping gene to normalize samples for the transcription analysis.

Western Blotting of Protein Expression

For protein extraction, cerebrocortical powder samples were homogenized in HEPES lysis buffer composed of 50 mM HEPES (pH 7.4), 150 mM NaCl, 1.5 mM $MgCl_2$, 1 mM EGTA, 10% (w/w) glycerol, 1 mM DTT, 50 mM NaF, and 10 mM Na-pyrophosphate. All products were obtained from Sigma-Aldrich. The lysate was centrifuged at 15,000×*g* for 15 min, and protein quantification was carried out in the supernatant using BCA protein assay (Pierce, Rockford, IL, USA).

For Western blotting, equal amounts of proteins were dissolved in loading sample buffer under reducing conditions, separated by 12% SDS-PAGE, and transferred to 0.2-μm nitrocellulose membranes. Immunolabeling was carried out with the following primary antibodies from Cell Signaling Technology (Beverly, MA, USA), diluted as 1/1000: anti-NF-κB p65 (ref. 8242), anti-phospho-NF-κB p65 (Ser 536) (ref. 3039), anti-STAT3 (ref. 4904), anti-phospho-STAT3 (Tyr 705) (ref. 9145), anti-Bax (ref. 2772), anti-Bcl-2 (ref. 2762S), and anti-caspase 3 (ref. 9662S). Anti-β-actin mouse monoclonal antibody (1/10000, Sigma-Aldrich, ref. A1978) was used as housekeeping protein. Membranes were incubated for 1 h at room temperature with the appropriate HRP-linked secondary antibody (1 : 5000) (Cell Signaling Technology). Blots were visualized using a chemiluminescence detection kit ECL western blotting substrate (Fisher Scientific, Barcelona, Spain), and the signals were captured using a ChemiDoc™ XRS + Imaging System (Bio-Rad).

Table 2 Oligonucleotides used for RT-qPCR

Target gene	TaqMan® probe or direct/reverse oligonucleotide
Tnfa	Rn01525859_g1
Il6	Rn01410330_m1
Il1b	Rn00580432_m1
Actb	Rn00667869_m1
Vegfa	5′-GTACCTCCATGCCAAGT-3′ 5′-CACTCCAGGGCTTCATCATT-3′
Mmp9	5′-CCAGCATCTGTATGGTCGTG-3′ 5′-AGCAGTAGGGGGACCTGTG-3′
Timp1	5′-GCACAGTGTTTCCCTGTTCA-3′ 5′-GTCATCGAGACCCCAAGGTA-3′
Sod1	5′-CACTTCGAGCAGAAGGCAAG-3′ 5′-CTGGACCGCCATGTTTCTTA-3′
Sod2	5′-GGCCAAGGGAGATGTTACAA-3′ 5′-GAACCTTGGACTCCCACAGA-3′
Cat	5′-CTCAGAAACCCGATGTCCTG-3′ 5′-GCTCCCTTTGCATGTACCAC-3′
Socs3	5′-TGCAGGAGAGCGGATTCTAC-3′ 5′-GCACTGGATGCGTAGGTTCT-3′
Actb	5′-TTCAACACCCCAGCCATGT-3′ 5′-GTGGTACGACCAGAGGCATACA-3′

Determination of Malondialdehyde

Malondialdehyde (MDA), a lipid peroxidation end product, was determined in cerebral cortex according to the modified method based in the thiobarbituric acid reactive species (TBARS) [37]. Briefly, the supernatant (50 μl) of tissue homogenate was mixed with 500 μl of TBA (0.2%)-AcOH 2 M (pH 3.5). Then, samples were incubated for 60 min at 95 °C. After cooling, the precipitate was removed by centrifugation at 1000 rpm for 10 min. The reaction product (TBA_2–MDA complex) was measured at 532 nm in a Multiskan Spectrum spectrophotometer (Fisher Scientific). The MDA concentration of the sample was calculated using an extinction coefficient of $1.56 \times 105\ M^{-1}\ cm^{-1}$ and expressed relative to total lipids.

Immunohistochemistry

Rats were euthanized, the brain removed, flash-frozen, and cut into sections (18 μm) in the coronal plane (0.2 to − 1.8 mm from bregma), which were fixed on glass slides. Endogenous peroxidase was inhibited for 30 min with 3% H_2O_2 in PBS, and tissue was permeabilized with sodium citrate buffer pH 6. Non-specific binding was blocked for 1 h with 10% normal goat serum (Sigma-Aldrich, ref. NS02L). The sections were washed with cold PBS containing 0.1% Tween-20 and bound with the Iba-1 primary antibody (ref. 019-19741; Wako,

Richmond, VA, USA), incubated at 4 °C overnight. Biotinylated anti-rabbit IgG antibody (BA-1000, Vector Laboratories, Burlingame, CA, USA) was incubated for 1 h at room temperature. After secondary antibody incubation, sections were washed with PBS and then incubated for 30 min with avidin–biotin complex kit (PK6100, Vector Laboratories) and stained using SIGMAFAST 3,3′-diaminobenzidine tablets (Sigma-Aldrich). Sections were then rinsed in water, dried, and coverslipped with Entellan (Merck, Darmstadt, Germany). Sections were visualized through a Leica DM 4500B microscope (Leica Microsystems, Barcelona, Spain) and acquired with a Leica DFC300FX camera (Leica Microsystems).

TUNEL Detection of DNA Cleavage and Caspase Activity Assay

Apoptotic DNA fragmentation was assessed in the cortex of rat brain sections (18 μm) by terminal deoxynucleotidyl transferase-mediated dUTP nick end labeling (TUNEL), by following manufacturer's instructions (In Situ Cell Death Detection Kit, Roche Molecular Biochemicals, Mannheim, Germany). Then, nuclei were stained using DAPI (1:5000, Molecular Probes, Eugene, OR, USA).

Caspase activity was assessed by the specific APO LOGIX™ FAM caspase detection kit (Cell Technology, Mountain View, CA, USA), as previously described [38]. In situ caspase-3 activity was assessed by labeling with FAM-DEVD-FMK, a relatively selective inhibitor of caspase-3 [39]. Sections were dry-mounted and coverslipped with ProLong (Molecular Probes) to reduce fluorescence quenching.

Images were viewed through a fluorescence microscope Leica DM 4500B (Leica Microsystems) and acquired with a Leica DFC 300 FX camera with Leica Application Suite V4. ImageJ NIH program was used for image analysis. The number of TUNEL-positive cells was expressed as a percentage of the corresponding DAPI-positive cells, and for quantitation of caspase-3 activity, the fluorescence was expressed relative to the field area, as usually done in our laboratory [38, 40, 41].

Statistical Analysis

Data are expressed as mean ± SEM, except for neurofunctional scores that are median with the first and third quartiles. Data analysis was performed using GraphPad Prism 6 software (GraphPad Software, CA, USA).

Statistical comparisons were carried out for body weight (unpaired Student's *t* test); hemodynamic parameters and core temperature (two-way ANOVA, with treatment and tMCAO stage as independent factors); plasma UA levels (two-way ANOVA, with treatment and time after tMCAO as independent factors, followed by post hoc Holm-Sidak's multiple comparisons test); cerebrocortical UA concentration (two-way ANOVA, with treatment and brain hemisphere as independent factors, followed by post hoc Holm-Sidak's multiple comparisons test); neurofunctional score (Mann-Whitney test); total brain infarct and edema volumes (unpaired Student's *t* test); cortical/subcortical infarct sizes (two-way ANOVA, with treatment and brain area as independent factors, followed by post hoc Fisher multiple comparisons test); mRNA expressions and MDA levels (two-way ANOVA, with treatment and brain hemisphere as independent factors, followed by post hoc Holm-Sidak's multiple comparisons test); and apoptosis biomarkers (unpaired Student's *t* test). Differences were considered significant at $P < 0.05$.

Results

Body Weight, Physiological Parameters, and Uric Acid Levels

Body weight values were similar in the two experimental groups: vehicle-treated and UA-treated rats. The reduction of CP during ischemia was comparable in the two groups, as was the extent of perfusion increase during reperfusion. Mean arterial blood pressure, core temperature, and serum glucose were in the physiologic range, remained stable along the ischemia-reperfusion procedure, and were similar in the two experimental groups (Table 3).

Plasma UA levels in rats subjected to tMCAO were 0.49 ± 0.13 mg/dL at reperfusion and did not significantly change during the following 6 h. Intravenous UA injection (16 mg/kg), 20 min after the end of tMCAO, produced a significantly ($P < 0.01$) dramatic increase in plasma UA levels at 2 h, which decreased at 4 h, and returned to basal levels at 6 h of reperfusion (Fig. 2a). Cerebrocortical UA concentration was similar in the ipsilateral ischemic hemisphere (233 ± 47 ng/mg protein) and the contralateral hemisphere (174 ± 34 ng/mg protein) of vehicle-treated rats at 6 h after tMCAO. At this time point, UA concentration was not significantly modified in the contralateral hemisphere of UA-treated rats (203 ± 56 ng/mg protein). By contrast, UA concentration significantly increased in the ipsilateral ischemic hemisphere of UA-treated rats (727 ± 73 ng/mg protein), when compared with both the contralateral hemisphere of UA-treated rats ($P < 0.01$) and the ipsilateral ischemic hemisphere of vehicle-treated rats ($P < 0.01$).

Uric Acid Administration After tMCAO Improves Neurological Function and Reduces Brain Infarct Volume

Neurofunctional evaluation at 24 h after tMCAO showed significantly ($P < 0.01$) lower neurofunctional impairment scores

Table 3 Sample characteristics of the experimental groups

	Vehicle ($n = 13$)			Uric acid ($n = 13$)		
	Basal	Ischemia	Reperfusion	Basal	Ischemia	Reperfusion
Body wt (g)	327.46 ± 6.47	-	-	310.54 ± 6.02	-	-
CP (%)	100	40.56 ± 3.85	134.99 ± 14.35	100	43.38 ± 3.67	168.23 ± 22.24
MABP (mm Hg)	133.39 ± 3.09	124.23 ± 3.05	131.90 ± 3.74	118.21 ± 3.09	129.13 ± 3.71	134.90 ± 4.25
Temperature (°C)	36.56 ± 0.26	35.90 ± 0.23	36.30 ± 0.27	36.15 ± 0.24	36.63 ± 0.17	35.53 ± 0.25
Glycemia (mg/dL)	124.46 ± 10.27	115.23 ± 6.81	123.38 ± 7.69	121.85 ± 11.42	124.77 ± 7.37	134.46 ± 14.13

Data are presented as mean ± SEM

CP cortical perfusion, *MABP* mean arterial blood pressure

in UA-treated rats, when compared with vehicle-treated rats (Fig. 2b). In accordance with improved neurofunctional outcome, UA treatment reduced the size of brain infarct (Fig. 2c). Total infarct volume, corrected for edema, significantly ($P < 0.05$) decreased from 29.53 ± 5.14% of the ipsilateral ischemic hemisphere in vehicle-treated rats to 17.89 ± 3.56% in UA-treated rats. There was a region-selective protective effect of UA, which significantly ($P < 0.05$) reduced infarct volume of the cortical region rather than the subcortical region (Fig. 2d).

Uric Acid Treatment Reduces tMCAO-Induced Early *Vegfa* Overexpression and Subsequent Brain Edema

In addition to the reduction of cortical infarct, UA administration significantly ($P < 0.05$) reduced brain edema volume at 24 h after tMCAO (Fig. 3a). To elucidate molecular mechanisms involved in the effects of UA on brain edema, we examined the time course of expression levels of *Vegfa*, *Mmp9*, and *Timp1* genes in brain cortex.

Vegfa mRNA levels significantly ($P < 0.01$) increased in the ipsilateral ischemic hemisphere at 6 h after tMCAO, when compared with the contralateral hemisphere of vehicle-treated rats. By contrast, this increase was not observed in UA-treated rats (Fig. 3b). On the other hand, expression levels of *Vegfa* were similar in the ipsilateral and contralateral hemispheres of vehicle-treated rats at 24 h after tMCAO. However, at this time point, UA treatment induced a significant ($P < 0.01$) *Vegfa* overexpression in the ipsilateral ischemic hemisphere (Fig. 3b).

Mmp9/*Timp1* expression ratio was significantly ($P < 0.05$) increased in the ipsilateral ischemic hemisphere at 24 h after tMCAO, when compared with 6 h after the transient ischemic insult. Interestingly, UA treatment significantly ($P < 0.01$) decreased the rise in *Mmp9*/*Timp1* expression ratio at 24 h after tMCAO, when compared with vehicle treatment (Fig. 3c).

Uric Acid Treatment Is Associated to IL-6/STAT3 Activation After tMCAO

In order to profile the inflammatory response in the cortex of ischemic brain, we first analyzed the mRNA expression levels of *Il6*, *Tnfa* and *Il1b* cytokine genes after tMCAO. Transient ischemia induced significant ($P < 0.05$) upregulation of *Tnfa* and *Il1b* mRNA expression, both at 6 h and 24 h, in the ipsilateral ischemic hemisphere, when compared with the contralateral hemisphere. By contrast, a significant ($P < 0.01$) increase in *Il6* expression was only observed at 24 h post-tMCAO (Fig. 4a). Interestingly, UA-treated rats exhibited a significantly ($P < 0.01$) dramatic increase of *Il6* expression in the ipsilateral ischemic hemisphere at 6 h after tMCAO, a significant ($P < 0.01$) decrease in *Tnfa* expression at 24 h, and no significant change in *Il1b* expression, when compared with vehicle-treated rats (Fig. 4a).

Levels of phospho-STAT3, a transcription factor dependent on IL-6, were analyzed as a possible neuroprotective pathway. Although tMCAO elicited a slight increase of phospho-STAT3 levels in the ipsilateral ischemic hemisphere, when compared with the contralateral hemisphere, it is noteworthy that UA treatment triggered an intense upregulation of phospho-STAT3 protein at 6 h and 24 h after the transient ischemic insult (Fig. 4b). In close relation to IL-6/STAT3 signaling pathway, we studied *Socs3* mRNA expression, a negative regulator of cytokine signaling. Again, although transient ischemia significantly ($P < 0.05$) increased *Socs3* mRNA at both 6 h and 24 h, UA-treated rats exhibited a remarkable induction of *Socs3* gene expression at 24 h after tMCAO in the ipsilateral ischemic hemisphere, significantly ($P < 0.01$) higher than in vehicle-treated rats (Fig. 4c).

Western blot analysis also showed changes in phosphorylation levels at the Ser536 site located in the transactivation domain of the p65 subunit of transcription factor NF-κB, a master regulator of the inflammatory response. There was a slight increase of phospho-p65 levels in the ipsilateral ischemic hemisphere at 6 h after tMCAO, when compared with the

contralateral hemisphere. On the other hand, at this time point, there were markedly enhanced levels of phospho-p65 in the contralateral hemisphere and, to a higher extent, in the ipsilateral ischemic hemisphere of UA-treated rats (Fig. 4d). However, at 24 h after tMCAO, levels of phospho-p65 were higher in ipsilateral ischemic hemispheres, when compared with contralateral hemispheres, in both vehicle-treated and UA-treated rats (Fig. 4d).

Moreover, we evaluated the activation of microglia, given its central role in neuroinflammation. Immunohistochemical analysis of Iba-1, a microglia-specific calcium-binding protein, showed reactive amoeboid shaped microglia at 24 h after tMCAO in the ipsilateral ischemic hemisphere of vehicle-treated rats. By contrast, quiescent ramified microglia was observed in UA-treated rats (Fig. 4e).

Uric Acid Treatment Enhances Antioxidant Defense Gene Expression to Reduce Lipid Peroxidation After tMCAO

In order to assess whether UA-driven induction of IL-6/STAT3 pathway modulated transcriptional activity of antioxidant defense genes to control the levels of ROS associated with ischemic stroke, we evaluated *Sod1*, *Sod2*, and *Cat*

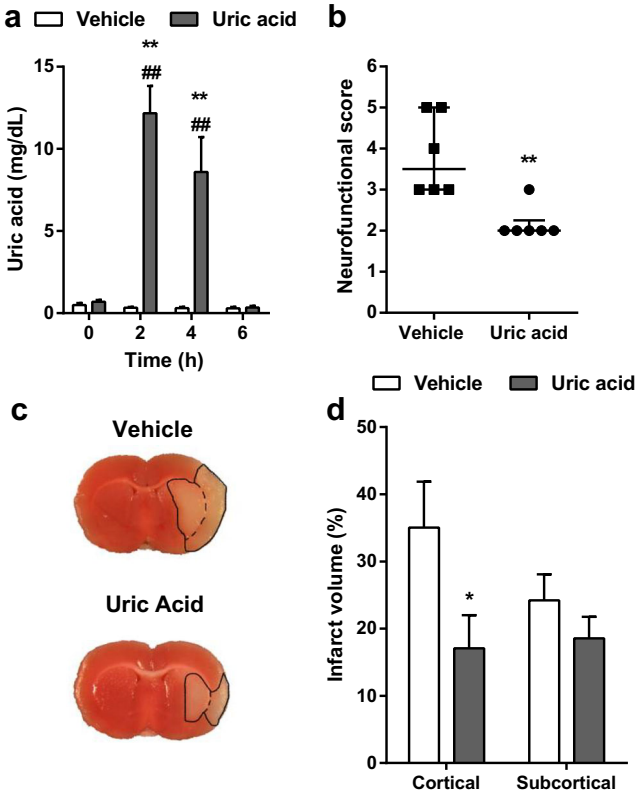

Fig. 2 Effects of uric acid (UA) administration on neurological function and brain infarct volume after ischemic stroke in rats subjected to tMCAO. **a** Time course of plasma UA levels after tMCAO. **Significantly different from vehicle, $P < 0.01$; ##significantly different from 0 h time, $P < 0.01$ (two-way ANOVA). **b** Severity of neurofunctional deficits, 24 h after tMCAO, scored with four tests assessing spontaneous activity, circling to the left, parachute reflex symmetry, and resistance to left forepaw stretching. **Significantly different from vehicle, $P < 0.01$ (Mann-Whitney test). **c** Representative images showing cortical and subcortical brain infarct (pale areas) in TTC-stained 2-mm-thick brain coronal sections (0.2 to − 1.8 mm from bregma), 24 h after tMCAO. **d** Brain infarct volume calculated with edema correction, separately for cortical and subcortical regions, as determined by morphometric analysis of seven 2-mm-thick TTC-stained coronal sections. *Significantly different from vehicle, $P < 0.05$ (two-way ANOVA). tMCAO transient middle cerebral artery occlusion. TTC 2,3,5-triphenyltetrazolium chloride. Plasma UA levels and infarct volume data are mean ± SEM, and neurofunctional scores are median with the first and third quartiles, from 4–6 vehicle-treated and 4–6 UA-treated rats

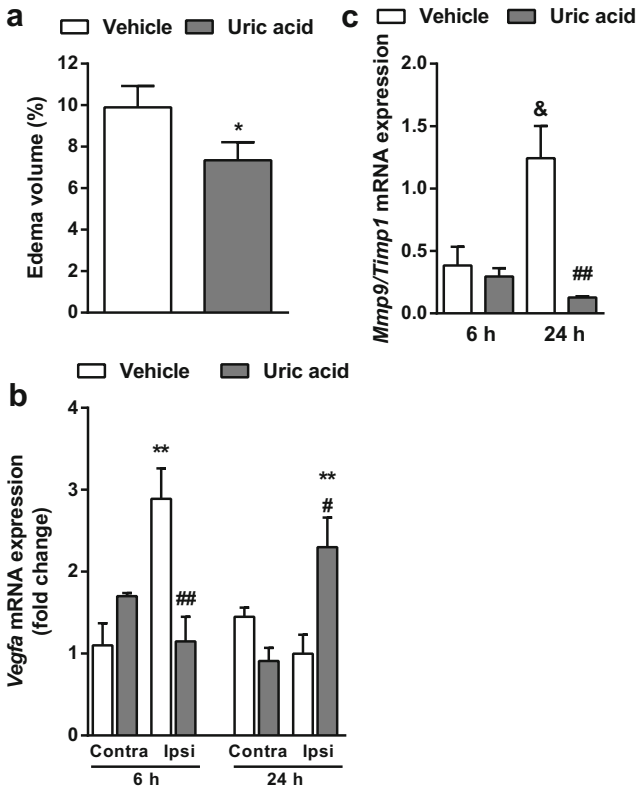

Fig. 3 Effects of uric acid (UA) administration on brain edema volume and expression of genes involved in brain swelling after ischemic stroke in rats subjected to tMCAO. **a** Brain edema volume, 24 h after tMCAO, determined as the subtraction between raw and edema-corrected infarcted hemisphere by morphometric analysis of seven 2-mm thick TTC-stained coronal sections. *Significantly different from vehicle, $P < 0.05$ (unpaired Student's *t* test). **b** Time course of *Vegfa* gene expression in brain cortex. *Vegfa* mRNA levels were determined by RT-qPCR analysis, using *Actb* as housekeeping gene. **Significantly different from contralateral non-ischemic cortex, $P < 0.01$; #significantly different from vehicle, $P < 0.05$; and ##significantly different from vehicle, $P < 0.01$ (two-way ANOVA). **c** Time course of *Mmp9*/*Timp1* gene expression ratio in ischemic brain cortex. *Mmp9* and *Timp1* mRNA levels were determined by RT-qPCR analysis, using *Actb* as housekeeping gene. &Significantly different from 6 h after tMCAO, $P < 0.05$; and ##significantly different from vehicle, $P < 0.01$ (two-way ANOVA). tMCAO transient middle cerebral artery occlusion. TTC 2,3,5-triphenyltetrazolium chloride. Data are mean ± SEM from 4–6 vehicle-treated and 4–6 UA-treated rats

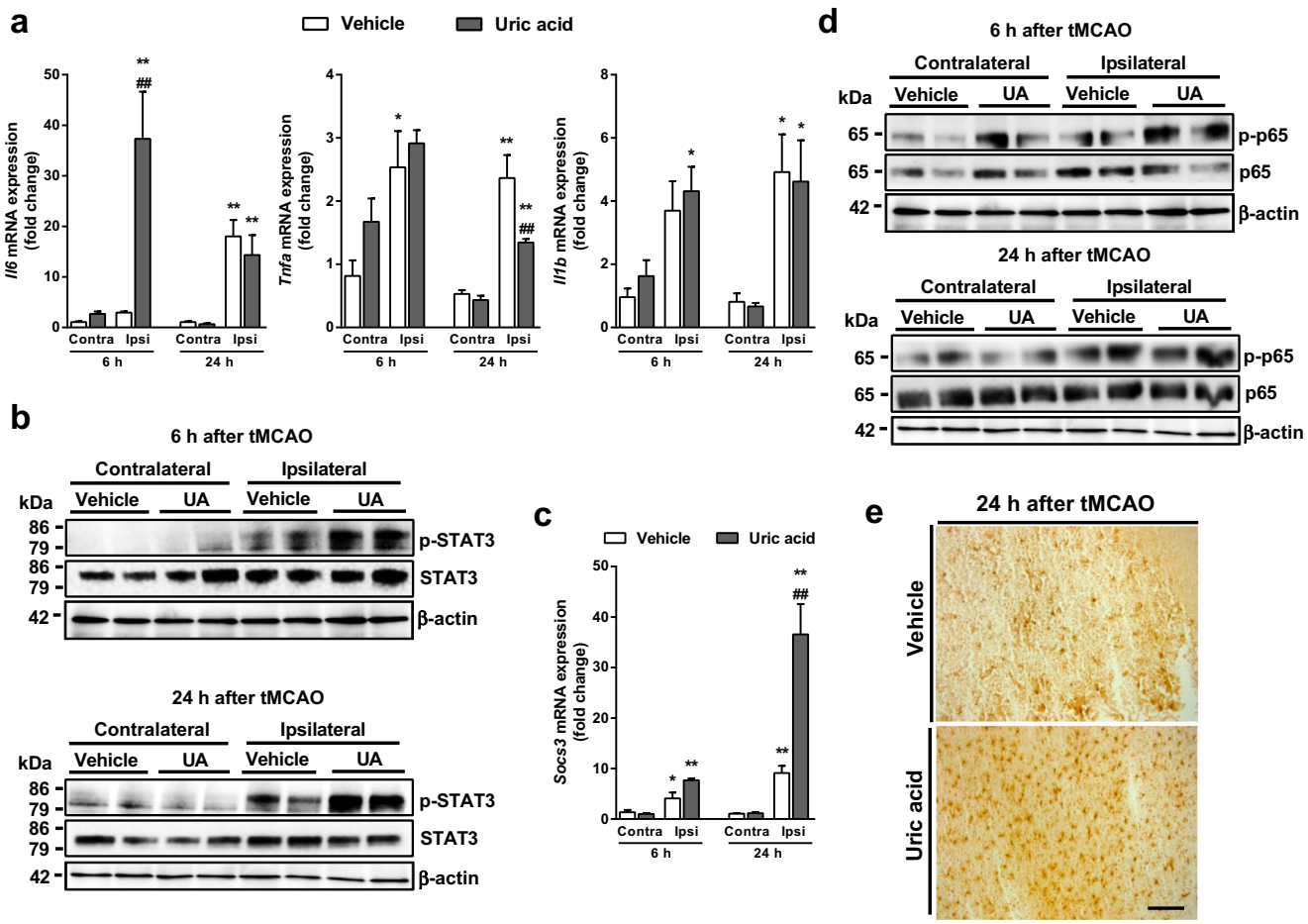

Fig. 4 Effects of uric acid (UA) administration on brain expression of cytokine genes, transcription factor proteins, and cytokine transcription regulator gene, as well as microglia activation after ischemic stroke in rats subjected to tMCAO. **a** Time course of *Il6*, *Tnfa*, and *Il1b* gene expressions in brain cortex. Cytokine mRNA levels were determined by RT-qPCR analysis, using *Actb* as housekeeping gene. *Significantly different from contralateral non-ischemic cortex, $P < 0.05$; **significantly different from contralateral non-ischemic cortex, $P < 0.01$; and $^{\#\#}$significantly different from vehicle, $P < 0.01$ (two-way ANOVA). **b** Representative images of p-STAT3 protein expression time course, relative to total STAT3, in brain cortex. Protein expression was shown by Western blotting, using β-actin as housekeeping protein for loading control. **c** Time course of *Socs3* gene expression in brain cortex. *Socs3* mRNA levels were determined by RT-qPCR analysis, using *Actb* as housekeeping gene. *Significantly different from contralateral non-ischemic cortex, $P < 0.05$; **significantly different from contralateral non-ischemic cortex, $P < 0.01$; and $^{\#\#}$significantly different from vehicle, $P < 0.01$ (two-way ANOVA). **d** Representative images of p-p65 protein expression time course, relative to total p65, in brain cortex. Protein expression was shown by Western blotting, using β-actin as housekeeping protein for loading control. **e** Representative photomicrographs of microglia appearance in ischemic cortex, 24 h after tMCAO (Scale bar = 100 μm). Reactive amoeboid shaped and quiescent ramified microglia were shown by immunohistochemical staining of the microglia-specific calcium-binding protein Iba-1. tMCAO transient middle cerebral artery occlusion. Data are mean ± SEM from 4–6 vehicle-treated and 4–6 UA-treated rats

mRNA expression. Neither the transient ischemic insult nor the UA treatment modified the cerebrocortical expression of these antioxidant defense genes at 6 h after tMCAO. UA treatment significantly ($P < 0.05$) enhanced expression of *Sod2* and *Cat* genes in the ipsilateral ischemic hemisphere at 24 h post-tMCAO, when compared with vehicle treatment (Fig. 5a). Then, in order to assess the effects of UA-elicited overexpression of antioxidant defense genes on oxidative damage, malondialdehyde (MDA) was measured as a lipid peroxidation biomarker. In accordance with the time course of *Sod2* and *Cat* transcriptional data, UA administration significantly ($P < 0.01$) restrained the elevated MDA levels induced by the transient ischemic insult in the ipsilateral hemisphere of vehicle-treated rats at 24 h after tMCAO (Fig. 5b).

Uric Acid Treatment Diminishes tMCAO-Driven Apoptosis by Modulating the Expression of Key Regulatory and Executioner Proteins

Since apoptosis is involved in ischemic brain damage, we also investigated the modulatory effect of UA on key regulators/executioners of the cell death program and on resulting apoptosis in brain cortex. As expected, western blotting at 24 h after tMCAO revealed reduced levels of the anti-apoptotic

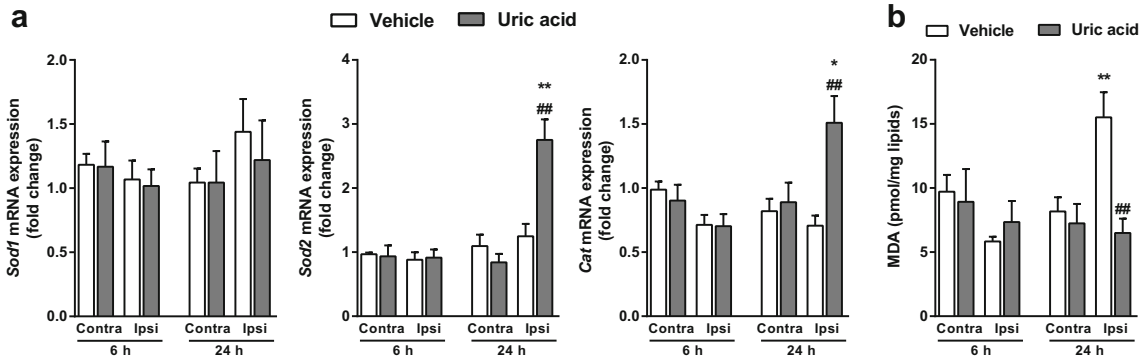

Fig. 5 Effects of uric acid (UA) administration on the brain expression of antioxidant defense genes and lipid peroxidation after ischemic stroke in rats subjected to tMCAO. **a** Time course of *Sod1*, *Sod2* and *Cat* gene expressions in brain cortex. Antioxidant enzyme mRNA levels were determined by RT-qPCR analysis, using *Actb* as housekeeping gene. *Significantly different from contralateral non-ischemic cortex, $P < 0.05$; **significantly different from contralateral non-ischemic cortex, $P < 0.01$; and ##significantly different from vehicle, $P < 0.01$ (two-way ANOVA). **b** Time course of the lipid peroxidation biomarker malondialdehyde (MDA) content in brain cortex. MDA levels were determined by the method based in the thiobarbituric acid reactive species (TBARS). **Significantly different from contralateral non-ischemic cortex, $P < 0.01$; and ##significantly different from vehicle, $P < 0.01$ (two-way ANOVA). tMCAO transient middle cerebral artery occlusion. Data are mean ± SEM from 4–6 vehicle-treated and 4–6 UA-treated rats

protein Bcl-2, increased levels of the proapoptotic protein Bax, and increased levels of the apoptosis executioner protease cleaved caspase-3 in the ipsilateral ischemic hemisphere of vehicle-treated rats, when compared with the contralateral hemisphere (Fig. 6a). Carboxyfluorescein in situ labeling confirmed activation of capase-3 in the ipsilateral ischemic hemisphere of vehicle-treated rats at this time point (Fig. 6b). Interestingly, UA treatment induced the expression of Bcl-2 and reduced the levels of Bax, as well as of cleaved caspase-3, when compared with vehicle treatment (Fig. 6a). Again, a significant ($P < 0.05$) inhibitory effect of UA on caspase-3 activation was confirmed by in situ labeling (Fig. 6b). With regard to cell apoptosis execution, the presence of TUNEL-positive nuclei observed at 24 h after tMCAO in the ipsilateral ischemic hemisphere of UA-treated rats was significantly ($P < 0.01$) lower than in the corresponding hemisphere of vehicle-treated rats (Fig. 6c).

Discussion

In this study, male Wistar rats subjected to transient ischemic stroke benefited from i.v. uric acid (UA) treatment administered early after reperfusion. Rats receiving UA showed reduced infarct and edema volumes, less brain apoptosis, and improved neurofunctional status. Our group and others have previously demonstrated neuroprotective properties of exogenous UA in ischemic stroke using different rodent models [4–11]. However, the mechanisms responsible for this beneficial effect are not yet completely elucidated. We now show, for the first time, that UA favorably targets oxidative stress, neuroinflammation, brain swelling, and apoptotic cell death in the cortical region after tMCAO in association with IL-6/STAT3 neuroprotective signaling pathway.

How systemically administered UA reaches its brain targets in ischemic stroke models is a matter of debate. It has been suggested that UA is primarily a vasculoprotective compound and that this effect may be ultimately responsible for the overall neuroprotection and improved outcome shown in experimental studies [24]. Our results show that i.v. UA injection induced a transient increase in plasma UA levels, which peaked at 2 h and vanished at 6 h of reperfusion. Interestingly, systemic UA administration also induced a selective increase of UA concentration in the injured, but not in the healthy brain, 6 h after the ischemic insult. Therefore, UA indeed passed the functionally compromised blood–brain barrier (BBB), entered to the brain, and played its protective role in the ischemic area. A previous report also in rats subjected to tMCAO [10] showed that i.v. administered UA did not result in increased UA brain concentration, although measured at much earlier time points (10–30 min) when compared with the present study. Of note, methyl- and sulfur-containing analogs of UA with increased solubility were detected in the brain up to 120 min after i.v. administration to mice [42].

Our study analyzed the cerebrocortical mRNA expression levels of *Tnfa*, *Il6*, and *Il1b* cytokine genes after tMCAO and the effect of UA treatment. The ischemic insult increased the expression of *Tnfa* and *Il1b*, while UA reduced the expression of *Tnfa* but not of *Il1b*. Concomitant cortical expression of *Tnfa* and *Il1b* mRNAs has been reported as part of the neuroinflammatory response in transient focal ischemia [43], and downregulation of *Tnfa* by UA would therefore contribute to anti-inflammation. Most interestingly, in the present study, UA treatment induced marked upregulation of *Il6* gene expression in rats subjected to transient focal ischemia. Previous reports showed that permanent MCAO in rats induced *Il6* mRNA expression [44] and IL-6 bioactivity [45] in the ischemic hemisphere. Moreover, local i.c.v. IL-6

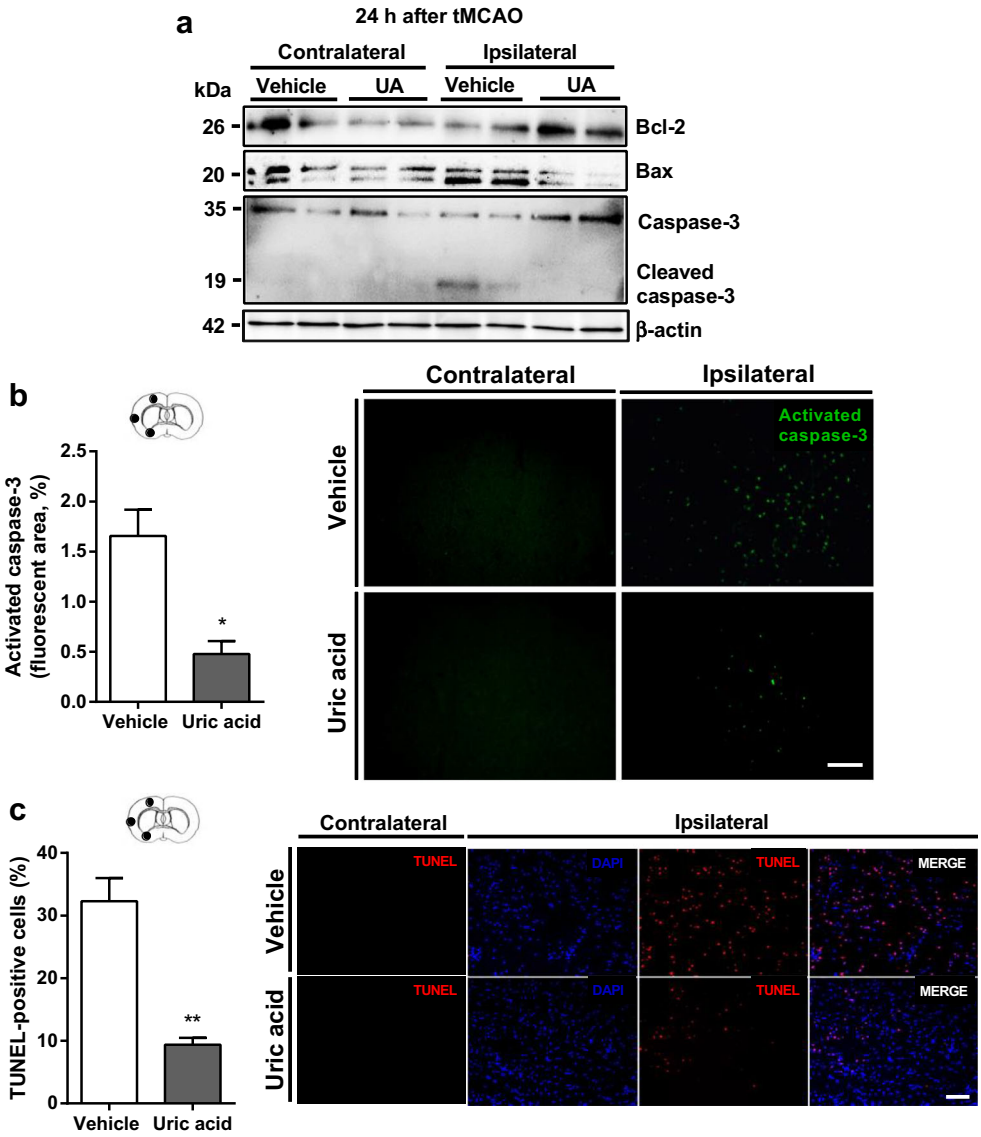

Fig. 6 Effects of uric acid (UA) administration on brain apoptotic cell death after ischemic stroke in rats subjected to tMCAO. **a** Representative images of antiapoptotic protein Bcl-2, proapoptotic protein Bax, and apoptosis executioner protease cleaved caspase-3 (relative to total caspase-3) expression in brain cortex. Protein expression was shown by Western blotting, using β-actin as housekeeping protein for loading control. **b** Quantification (average of three selected fields, black circle) and representative photomicrographs of activated caspase-3 positive cells, 24 h after tMCAO, as shown by carboxyfluorescein in situ labeling (Scale bar = 100 μm). *Significantly different from vehicle, $P < 0.05$ (unpaired Student's *t* test). **c** Quantification (average of three selected fields, black circle) and representative photomicrographs of apoptotic DNA fragmentation, 24 h after tMCAO, as shown by terminal deoxynucleotidyl transferase-mediated dUTP nick end labeling (TUNEL) (Scale bar = 100 μm). **Significantly different from vehicle, $P < 0.01$ (unpaired Student's *t* test). tMCAO transient middle cerebral artery occlusion. Data are mean ± SEM from 3 vehicle-treated and 3 UA-treated rats

infusion reduced ischemic brain damage after permanent MCAO in rats [45] and had a trophic effect on hippocampal neurons in gerbils subjected to forebrain ischemia [46]. The source for the increase in levels of IL-6 early after stroke has long been debated. After experimental cerebral ischemia, local upregulation of IL-6 has been a consistent finding, mostly not only in neurons but also in glial cells and vascular endothelium [47, 48]. Based on these in vivo premises, Gertz and colleagues attempted to identify the exact cellular source of IL-6 in brain after in vitro ischemia, using pure and mixed cell cultures, and organotypic brain slices [49]. They concluded that the upregulation of IL-6 expression in the brain after ischemia takes the form of a self-amplifying network response of all resident cells. In our study, UA could increase this network response, rather than acting on a single cell type.

Our results show that, in parallel to *Il6* mRNA upregulation, UA treatment also triggered an intense overexpression of cerebrocortical phospho-STAT3 transcription factor protein after the transient ischemic insult. Previous studies showed that neuroprotection by endogenous IL-6 is mediated by STAT3 activation after ischemic stroke in mice [29, 30]. Therefore, altogether, our results suggest a role for the IL-6/STAT3 signaling pathway in UA elicited reduction of ischemic brain damage after stroke in rats, which confirmation by using pathway inhibitors warrants further research. On the other hand, IL-6 receptor (IL-6R) is expressed in neurons and microglia [50, 51], but not in astrocytes [50]. Considering that IL-6 promotes STAT3 phosphorylation through its binding to IL-6R, STAT3 activation is likely to occur in neurons rather than in microglia. In fact, the blockade of IL-6 signaling exacerbated ischemic cerebral damage in mice through the reduction in p-STAT3 in peri-infarct cortical neurons [29]. By contrast, UA could reduce brain damage by activating the IL-6/STAT3 pathway in neurons, in line with

neuronal STAT3 activation mediating neuroprotection induced by estradiol [52] and the PPAR-γ agonist pioglitazone [53] after ischemic stroke.

NF-κB is another well-characterized transcription factor with dual roles in cell death and survival in neurological disorders and implications in neuroprotective therapy [54]. In the present study, we measured levels of total p65 and phospho-p65 (Ser536) subunit of NF-κB in whole tissue extract. Phosphorylation of the Ser536 site—located in the p65 transactivation domain—is considered one of the most important inducible phosphorylations of NF-κB [55], and it has been associated with its nuclear translocation and with the transcriptional activation of its target genes [56–59]. Here, we report enhanced levels of phospho-p65 (Ser536) subunit of the transcription factor NF-κB in the ipsilateral ischemic hemisphere of UA-treated rats compared with vehicle-treated rats, at 6 h but not at 24 h after transient ischemia. These results support a selective transient activation of NF-κB in the injured brain of UA-treated rats after ischemic stroke. It is known that persistent neuronal NF-κB activation contributes to cerebral ischemic damage after permanent MCAO [60]. However, transient NF-κB signaling in cerebral ischemia is also responsible for beneficial effects [61] such as preconditioning development [62] and apoptosis inhibition [63]. Indeed, NF-κB activation enhances anti-apoptotic protein levels and thus promotes neuron survival [64]. On the other hand, diminished oxidative stress increases NF-κB related rapid defenses, such as immune response and anti-apoptotic factors, thus preventing brain damage after tMCAO [65]. We suggest that transient NF-kB activation elicited by UA may transcriptionally induce different immune factors such as the neuroprotective cytokine IL-6. In turn, high levels of IL-6 would induce STAT3 activation.

Interestingly, NF-κB and STAT3 cooperatively modulate the transcriptional regulation of a variety of anti-apoptotic genes [66]. On the other hand, nuclear translocation of STAT3 and NF-κB are independent of each other but NF-κB supports Il6-induced expression and activation of STAT3 [67]. Our data show that treatment with UA increased the cerebrocortical levels of both phospho-p65, subunit of NF-κB, and phospho-STAT3 after the transient ischemic insult. It has been reported that IL-32α exerts a neuroprotective role in mice subjected to tMCAO by cytokine signaling through both STAT3 and NF-κB pathways [68]. Similarly, our results support that the beneficial effects of UA associated with the IL-6/STAT3 signaling pathway also involve NF-κB activation.

Socs3 gene expression is activated by the IL-6/STAT3 signaling pathway [69], and SOCS3 protein is a transcription regulator with potential impact on cytokine production and microglia activation in neuropathological conditions including stroke [70]. The present study observed induction of cerebrocortical *Socs3* expression by tMCAO, in line with gene expression analysis after a similar ischemic insult in SHR rats [71] and mice [72]. Moreover, our results show a dramatic *Socs3* overexpression in UA-treated rats, thus supporting a role for the IL-6/STAT3/SOCS3 signaling pathway in neuroprotection by UA, in accordance with previous studies showing neuroprotective effects of SOCS3 induction in rodent ischemic stroke [71, 72].

Critical to the process of neuroinflammation is the role of microglia in pathological progression of ischemic tissue. In focal ischemia, the activated resident microglia proliferates and accumulates in the peri-infarct region, adapting an amoeboid morphology, instead of the characteristic ramified morphology of the inactive phenotype [73]. In our model, we have verified that UA administration maintains the ramified morphology of Iba-1-positive microglia in brain cortex, which suggests an anti-inflammatory role of UA during ischemia. However, beyond morphological transformation, reactive microglia display polarization functional phenotypes with beneficial or detrimental contributions to post-stroke recovery [74].

Restoration of blood flow in transient ischemic stroke contributes to overproduction of ROS, mainly by the mitochondria, and therefore to the presence of oxidative damage in brain tissue [75], setting the rationale for the use of antioxidants as neuroprotective therapy [76, 77]. Previous studies found that the neuroprotective capacity of UA in rat ischemic stroke was associated to reduced brain ROS production and decreased lipid, protein, and DNA oxidative stress biomarkers [7, 10, 11, 25]. Our results show that UA treatment enhances cerebrocortical *Sod2* and *Cat* gene expression after induction of stroke. In mice subjected to ischemic stroke, STAT3 modulates brain Mn-SOD (i.e., mitochondrial SOD2) expression and superoxide accumulation [78], and IL-6-induced STAT3 activation promotes Mn-SOD expression [30], thus supporting a role for the IL-6/STAT3 pathway in UA-induced expression of the first line defense antioxidant enzymes. This STAT3 role adds to recently reported involvement of Nrf2 transcription factor in UA-elicited protection against reperfusion oxidative stress in ischemic stroke [25]. We also observed a decrease in the levels of the lipid peroxidation biomarker MDA in the cortex of UA-treated rats, in line with the link between SOD/catalase and MDA levels reported in rats subjected to forebrain ischemia [79].

Free radicals are triggers of both cytotoxic and vasogenic edema after stroke, with VEGF and matrix metalloproteinases as recognized mediators of vasogenic brain swelling [80]. In the acute phase of ischemic stroke, VEGF-A is involved in the development of cerebral edema due to endothelial cell–cell junction breakdown and subsequent vascular leak [81]. Our results show that UA represses the induction of cerebrocortical *Vegfa* expression in the acute stage (6 h) of stroke, and thus, this would explain the reduced edema observed in rats subjected to UA treatment after the ischemic insult. Noteworthy, a recent study showed that UA neuroprotective treatment normalized the increased circulating VEGF-A levels and BBB breakdown

after ischemic stroke in SHR rats and reduced VEGF-A levels in hypertensive acute ischemic stroke patients from the URICO-ICTUS trial [26]. Moreover, VEGF-A has a Janus face in stroke pathophysiology: after its transient detrimental effects in the acute phase, late increased VEGF-A promotes neuronal protection as well as angiogenesis and functional recovery [82–84]. Importantly, at 24 h after stroke onset, we observed that *Vegfa* gene expression was upregulated by UA administration, which might further contribute to the beneficial effects of UA by promoting VEGF-A-induced neuroprotection. Delayed VEGF treatment also enhances angiogenesis and recovery after ischemic stroke in neonatal [83] and adult [84] rats. Whether UA treatment beyond 24 h from stroke onset would have additional beneficial effects by inducing angiogenesis through the IL-6/STAT3/VEGF-A signaling pathway [85] deserves further research.

VEGF-induced increase in BBB permeability in acute ischemic stroke is associated with upregulation of matrix metalloproteinases in rats [86, 87] and mice [88]. However, extracellular matrix homeostasis is maintained by a balance between proteolytic and anti-proteolytic factors [89], including MMP-9 and its natural inhibitor TIMP-1 [90, 91]. Because it is this balance that contributes to impairment of the BBB, the MMP-9/TIMP-1 ratio has been used to provide a closer assessment of the proteolytic potential of MMP-9 to degrade the extracellular matrix after ischemic stroke in rodents [92] and humans [93]. Interestingly, the increase of p-STAT3 triggered by neuroprotective leptin in cortical neurons after ischemic stroke is associated with an augmented expression of TIMP-1 [94]. Our data reveals that UA treatment decreases MMP-9/TIMP-1 ratio in brain cortex, thus suggesting that UA administration may contribute through early downregulation of the VEGF-A/MMP-9 pathway to restrict vascular permeability by improving BBB integrity in acute ischemic stroke.

Cell apoptosis plays a crucial role in the development of stroke brain damage in the ischemic penumbra, where the cell fate is determined by the expression of a number of proapoptotic and anti-apoptotic signaling proteins [95]. Among these proteins, upregulation of proapoptotic Bax and downregulation of anti-apoptotic Bcl-2 is a molecular landmark in neurons destined to apoptosis. On the other hand, caspase-3 is identified to act downstream Bax/Bcl-2 ratio and play a key role in apoptosis execution [96]. We have recently reported that blockade of caspase-3-induced apoptosis in involved in the beneficial effect of neuroprotective treatments for ischemic stroke [38, 40]. In the present study, the increased expression of Bax, decreased expression of Bcl-2, and activation of caspase-3 were detected in the cerebrocortical regions of animals subjected to ischemic stroke. However, UA treatment ameliorated the Bax/Bcl-2 ratio and consequently induced a reduction in cleaved caspase-3 and carboxyfluorescein in situ labeling of activated caspase-3, as well as a decrease in TUNEL-positive cell counts. Interestingly, STAT3 can promote cell survival by means of transcriptional regulation of apoptotic signaling proteins, such as the Bcl-2 family [97]. In rodent ischemic stroke, brain STAT3 activation by neuroprotective treatments has been associated with increased Bcl-2 expression and decreased caspase-3 activity [98], as well as with reduced number of TUNEL-positive cells [98, 99]. Therefore, the neuroprotective anti-apoptotic effect of UA could be due to activation of the IL-6/STAT3 signaling pathway.

In conclusion, the present study demonstrates for the first time that systemic (i.v.) UA treatment after ischemic stroke, which increases local UA concentration in the injured brain tissue, is associated to activation of the IL-6/STAT3 pathway, attenuation of VEGF-A/MMP-9 signaling, and modulation of relevant mediators of oxidative stress, neuroinflammation, and apoptotic cell death in brain cortex, thus leading to neuroprotection. Further research is warranted to identify the cell type/s targeted by UA. These findings extend the preclinical evidence supporting the neuroprotective effects of UA and point toward a multifaceted mechanism targeting ischemic stroke damage, with transcription factors such as STAT3 as key players. By targeting key steps of the ischemic cascade in a pleiotropic way, UA is a better adjunctive agent in endovascular treatments, compared with those based on monotargeted approaches. We are aware that these encouraging results should be confirmed in animals with stroke comorbidities, in females, and in old animals, to better model the human stroke population. Nonetheless, the present findings let us suggest that activation of the IL-6/STAT3 signaling pathway is a promising target in acute ischemic stroke therapy.

Acknowledgments The authors thank Javier Sicilia for his veterinary advice and Melisa Vera for her technical assistance in the IIS La Fe animal research facility.

Authors' Contributions Salvador Pérez, Juan B. Salom, Germán Torregrosa, and Ángel Chamorro contributed to the study conception and design. Experiments, data collection, and analysis were performed by Alicia Aliena-Valero, Sergio Rius-Pérez, and Júlia Baixauli-Martín. The first draft of the manuscript was written by Salvador Pérez and Juan B. Salom, and all authors commented on previous versions of the manuscript. All authors read and approved the final manuscript.

Funding This work was partially supported by RETICS research network INVICTUS+ from Spanish "Instituto de Salud Carlos III" (co-financed with European Regional Development Fund), through grant RD16/0019/0008.

Data Availability All data can be fully available upon reasonable request to the corresponding author.

Compliance with Ethical Standards

Disclaimer The funding source had no further role in study design; in the collection, analysis, and interpretation of data; in the writing the report; and in the decision to submit the paper for publication.

Competing Interests Ángel Chamorro is inventor of the patent "Pharmaceutical composition for neuroprotective treatment in patients with ictus comprising citicoline and uric acid" and whose proprietor is Hospital Clinic of Barcelona, Spain. The other authors declare no competing interests.

Ethics Approval Experiments were conducted in compliance with the legislation on protection of animals used for scientific purposes in Spain (RD 53/2013) and the EU (Directive 2010/63/EU). Protocols were approved by the Animal Experimentation Ethics Committee from IIS La Fe.

References

1. Becker BF (1993) Towards the physiological function of uric acid. Free Radic Biol Med 14:615–631. https://doi.org/10.1016/0891-5849(93)90143-I
2. Waring WS, Webb DJ, Maxwell SRJ (2001) Systemic uric acid administration increases serum antioxidant capacity in healthy volunteers. J Cardiovasc Pharmacol 38:365–371. https://doi.org/10.1097/00005344-200109000-00005
3. Cutler RG, Camandola S, Feldman NH, Yoon JS, Haran JB, Arguelles S, Mattson MP (2019) Uric acid enhances longevity and endurance and protects the brain against ischemia. Neurobiol Aging 75:159–168. https://doi.org/10.1016/j.neurobiolaging.2018.10.031
4. Yu ZF, Bruce-Keller AJ, Goodman Y, Mattson MP (1998) Uric acid protects neurons against excitotoxic and metabolic insults in cell culture, and against focal ischemic brain injury in vivo. J Neurosci Res 53:613–625. https://doi.org/10.1002/(SICI)1097-4547(19980901)53:5<613::AID-JNR11>3.0.CO;2-1
5. Justicia C, Salas-Perdomo A, Pérez-de-Puig I, Deddens LH, van Tilborg GAF, Castellví C, Dijkhuizen RM, Chamorro Á et al (2017) Uric acid is protective after cerebral ischemia/reperfusion in hyperglycemic mice. Transl Stroke Res 8:294–305. https://doi.org/10.1007/s12975-016-0515-1
6. Jiménez-Xarrié E, Pérez B, Dantas AP, Puertas-Umbert L, Martí-Fabregas J, Chamorro Á, Planas AM, Vila E et al (2018) Uric acid treatment after stroke prevents long-term middle cerebral artery remodelling and attenuates brain damage in spontaneously hypertensive rats. Transl Stroke Res. https://doi.org/10.1007/s12975-018-0661-8
7. Romanos E, Planas AM, Amaro S, Chamorro A (2007) Uric acid reduces brain damage and improves the benefits of rt-PA in a rat model of thromboembolic stroke. J Cereb Blood Flow Metab 27:14–20. https://doi.org/10.1038/sj.jcbfm.9600312
8. Dhanesha N, Vázquez-Rosa E, Cintrón-Pérez CJ, Thedens D, Kort AJ, Chuong V, Rivera-Dompenciel AM, Chauhan AK et al (2018) Treatment with uric acid reduces infarct and improves neurologic function in female mice after transient cerebral ischemia. J Stroke Cerebrovasc Dis 27:1412–1416. https://doi.org/10.1016/j.jstrokecerebrovasdis.2017.12.043
9. Aliena-Valero A, López-Morales MA, Burguete MC, Castelló-Ruiz M, Jover-Mengual T, Hervás D, Torregrosa G, Leira EC et al (2018) Emergent uric acid treatment is synergistic with mechanical recanalization in improving stroke outcomes in male and female rats. Neuroscience 388:263–273. https://doi.org/10.1016/j.neuroscience.2018.07.045
10. Onetti Y, Dantas AP, Pérez B, Cugota R, Chamorro A, Planas AM, Vila E, Jiménez-Altayó F (2015) Middle cerebral artery remodeling following transient brain ischemia is linked to early postischemic hyperemia: a target of uric acid treatment. Am J Physiol Heart Circ Physiol 308:H862–H874. https://doi.org/10.1152/ajpheart.00001.2015
11. Zhang B, Yang N, Lin S, Zhang F (2017) Suitable concentrations of uric acid can reduce cell death in models of OGD and cerebral ischemia–reperfusion injury. Cell Mol Neurobiol 37:931–939. https://doi.org/10.1007/s10571-016-0430-8
12. Chamorro Á, Obach V, Cervera Á et al (2002) Prognostic significance of uric acid serum concentration in patients with acute ischemic stroke. Stroke 33:1048–1052. https://doi.org/10.1161/hs0402.105927
13. Wang Z, Lin Y, Liu Y, Chen Y, Wang B, Li C, Yan S, Wang Y et al (2016) Serum uric acid levels and outcomes after acute ischemic stroke. Mol Neurobiol 53:1753–1759. https://doi.org/10.1007/s12035-015-9134-1
14. Lei Z, Cai J, Hong H, Wang Y (2019) Serum uric acid level and outcome of patients with ischemic stroke: a systematic review and meta-analysis. Neurologist 24:121–131. https://doi.org/10.1097/NRL.0000000000000234
15. Amaro S, Soy D, Obach V et al (2007) A pilot study of dual treatment with recombinant tissue plasminogen activator and uric acid in acute ischemic stroke. Stroke 38:2173–2175. https://doi.org/10.1161/STROKEAHA.106.480699
16. Amaro S, Obach V, Cervera A, Urra X, Gómez-Choco M, Planas AM, Chamorro Á (2009) Course of matrix metalloproteinase-9 isoforms after the administration of uric acid in patients with acute stroke: a proof-of-concept study. J Neurol 256:651–656. https://doi.org/10.1007/s00415-009-0153-6
17. Amaro S, Cánovas D, Castellanos M, Gállego J, Martí-Fàbregas J, Segura T, Chamorro Á (2010) The Urico-Ictus Study, a phase 3 study of combined treatment with uric acid and rtPA administered intravenously in acute ischaemic stroke patients within the first 4.5 h of onset of symptoms. Int J Stroke 5:325–328. https://doi.org/10.1111/j.1747-4949.2010.00448.x
18. Chamorro Á, Amaro S, Castellanos M, Segura T, Arenillas J, Martí-Fábregas J, Gállego J, Krupinski J et al (2014) Safety and efficacy of uric acid in patients with acute stroke (URICO-ICTUS): a randomised, double-blind phase 2b/3 trial. Lancet Neurol 13:453–460. https://doi.org/10.1016/S1474-4422(14)70054-7
19. Amaro S, Laredo C, Renú A, Llull L, Rudilosso S, Obach V, Urra X, Planas AM et al (2016) Uric acid therapy prevents early ischemic stroke progression: a tertiary analysis of the URICO-ICTUS trial (Efficacy study of combined treatment with uric acid and r-tPA in acute ischemic stroke). Stroke 47:2874–2876. https://doi.org/10.1161/STROKEAHA.116.014672
20. Llull L, Laredo C, Renú A, Pérez B, Vila E, Obach V, Urra X, Planas A et al (2015) Uric acid therapy improves clinical outcome in women with acute ischemic stroke. Stroke 46:2162–2167. https://doi.org/10.1161/STROKEAHA.115.009960
21. Amaro S, Llull L, Renú A, Laredo C, Perez B, Vila E, Torres F, Planas AM et al (2015) Uric acid improves glucose-driven oxidative stress in human ischemic stroke: uric acid in ischemic stroke. Ann Neurol 77:775–783. https://doi.org/10.1002/ana.24378
22. Chamorro Á, Amaro S, Castellanos M, Gomis M, Urra X, Blasco J, Arenillas JF, Román LS et al (2017) Uric acid therapy improves the outcomes of stroke patients treated with intravenous tissue plasminogen activator and mechanical thrombectomy. Int J Stroke 12:377–382. https://doi.org/10.1177/1747493016684354
23. Amaro S, Renú A, Laredo C, Castellanos M, Arenillas JF, Llull L, Rudilloso S, Urra X et al (2019) Relevance of collaterals for the success of neuroprotective therapies in acute ischemic stroke: insights from the randomized URICO-ICTUS trial. Cerebrovasc Dis 47:171–177. https://doi.org/10.1159/000500712
24. Amaro S, Jiménez-Altayó F, Chamorro Á (2019) Uric acid therapy for vasculoprotection in acute ischemic stroke. Brain Circ 5:55–61. https://doi.org/10.4103/bc.bc_1_19
25. Ya B-L, Liu Q, Li H-F, Cheng HJ, Yu T, Chen L, Wang Y, Yuan LL et al (2018) Uric acid protects against focal cerebral ischemia/reperfusion-induced oxidative stress via activating Nrf2 and

regulating neurotrophic factor expression. Oxidative Med Cell Longev 2018:6069150–6069110. https://doi.org/10.1155/2018/6069150
26. Vila E, Solé M, Masip N, Puertas-Umbert L, Amaro S, Dantas AP, Unzeta M, D'Ocon P et al (2019) Uric acid treatment after stroke modulates the Krüppel-like factor 2-VEGF-A axis to protect brain endothelial cell functions: impact of hypertension. Biochem Pharmacol 164:115–128. https://doi.org/10.1016/j.bcp.2019.04.002
27. Ruggiero C, Cherubini A, Ble A, Bos AJG, Maggio M, Dixit VD, Lauretani F, Bandinelli S et al (2006) Uric acid and inflammatory markers. Eur Heart J 27:1174–1181. https://doi.org/10.1093/eurheartj/ehi879
28. Tanaka T, Milaneschi Y, Zhang Y, Becker KG, Zukley L, Ferrucci L (2017) A double blind placebo controlled randomized trial of the effect of acute uric acid changes on inflammatory markers in humans: a pilot study. PLoS One 12:e0181100. https://doi.org/10.1371/journal.pone.0181100
29. Yamashita T, Sawamoto K, Suzuki S, Suzuki N, Adachi K, Kawase T, Mihara M, Ohsugi Y et al (2005) Blockade of interleukin-6 signaling aggravates ischemic cerebral damage in mice: possible involvement of Stat3 activation in the protection of neurons. J Neurochem 94:459–468. https://doi.org/10.1111/j.1471-4159.2005.03227.x
30. Jung JE, Kim GS, Chan PH (2011) Neuroprotection by interleukin-6 is mediated by signal transducer and activator of transcription 3 and antioxidative signaling in ischemic stroke. Stroke 42:3574–3579. https://doi.org/10.1161/STROKEAHA.111.626648
31. Fisher M, Feuerstein G, Howells DW, Hurn PD, Kent TA, Savitz SI, Lo EH, STAIR Group (2009) Update of the Stroke Therapy Academic Industry Roundtable preclinical recommendations. Stroke 40:2244–2250. https://doi.org/10.1161/STROKEAHA.108.541128
32. Lapchak PA, Zhang JH, Noble-Haeusslein LJ (2013) RIGOR guidelines: escalating STAIR and STEPS for effective translational research. Transl Stroke Res 4:279–285. https://doi.org/10.1007/s12975-012-0209-2
33. Longa EZ, Weinstein PR, Carlson S, Cummins R (1989) Reversible middle cerebral artery occlusion without craniectomy in rats. Stroke 20:84–91. https://doi.org/10.1161/01.STR.20.1.84
34. Burguete MC, Torregrosa G, Pérez-Asensio FJ, Castelló-Ruiz M, Salom JB, Gil JV, Alborch E (2006) Dietary phytoestrogens improve stroke outcome after transient focal cerebral ischemia in rats. Eur J Neurosci 23:703–710. https://doi.org/10.1111/j.1460-9568.2006.04599.x
35. Bederson JB, Pitts LH, Germano SM, Nishimura MC, Davis RL, Bartkowski HM (1986) Evaluation of 2,3,5-triphenyltetrazolium chloride as a stain for detection and quantification of experimental cerebral infarction in rats. Stroke 17:1304–1308. https://doi.org/10.1161/01.STR.17.6.1304
36. Aliena-Valero A, Rius-Pérez S, Pérez S, Torregrosa G, Salom JB (2019) Optimised lyophilisation-based method for different biomolecule single-extractions from the same rat brain sample: suitability for RNA and protein expression analyses after ischemic stroke. J Neurosci Methods 327:108402. https://doi.org/10.1016/j.jneumeth.2019.108402
37. Ahmed MAE, El Morsy EM, Ahmed AAE (2014) Pomegranate extract protects against cerebral ischemia/reperfusion injury and preserves brain DNA integrity in rats. Life Sci 110:61–69. https://doi.org/10.1016/j.lfs.2014.06.023
38. López-Morales MA, Castelló-Ruiz M, Burguete MC, Jover-Mengual T, Aliena-Valero A, Centeno JM, Alborch E, Salom JB et al (2018) Molecular mechanisms underlying the neuroprotective role of atrial natriuretic peptide in experimental acute ischemic stroke. Mol Cell Endocrinol 472:1–9. https://doi.org/10.1016/j.mce.2018.05.014
39. Garcia-Calvo M, Peterson EP, Leiting B, Ruel R, Nicholson DW, Thornberry NA (1998) Inhibition of human caspases by peptide-based and macromolecular inhibitors. J Biol Chem 273:32608–32613. https://doi.org/10.1074/jbc.273.49.32608
40. Jover-Mengual T, Castelló-Ruiz M, Burguete MC, Jorques M, López-Morales MA, Aliena-Valero A, Jurado-Rodríguez A, Pérez S et al (2017) Molecular mechanisms mediating the neuroprotective role of the selective estrogen receptor modulator, bazedoxifene, in acute ischemic stroke: a comparative study with 17β-estradiol. J Steroid Biochem Mol Biol 171:296–304. https://doi.org/10.1016/j.jsbmb.2017.05.001
41. Burguete MC, Jover-Mengual T, López-Morales MA, Aliena-Valero A, Jorques M, Torregrosa G, Alborch E, Castelló-Ruiz M et al (2019) The selective oestrogen receptor modulator, bazedoxifene, mimics the neuroprotective effect of 17β-oestradiol in diabetic ischaemic stroke by modulating oestrogen receptor expression and the MAPK/ERK1/2 signalling pathway. J Neuroendocrinol 31:e12751. https://doi.org/10.1111/jne.12751
42. Haberman F, Tang S-C, Arumugam TV, Hyun DH, Yu QS, Cutler RG, Guo Z, Holloway HW et al (2007) Soluble neuroprotective antioxidant uric acid analogs ameliorate ischemic brain injury in mice. Neuromolecular Med 9:315–323. https://doi.org/10.1007/s12017-007-8010-1
43. Wang X, Yue TL, Barone FC, White RF, Gagnon RC, Feuerstein GZ (1994) Concomitant cortical expression of TNF-α and IL-1β mRNAs follows early response gene expression in transient focal ischemia. Mol Chem Neuropathol 23:103–114. https://doi.org/10.1007/bf02815404
44. Wang X, Yue TL, Young PR, Barone FC, Feuerstein GZ (1995) Expression of interleukin-6, c-fos, and zif268 mRNAs in rat ischemic cortex. J Cereb Blood Flow Metab 15:166–171. https://doi.org/10.1038/jcbfm.1995.18
45. Loddick SA, Turnbull AV, Rothwell NJ (1998) Cerebral interleukin-6 is neuroprotective during permanent focal cerebral ischemia in the rat. J Cereb Blood Flow Metab 18:176–179. https://doi.org/10.1097/00004647-199802000-00008
46. Matsuda S, Wen TC, Morita F, Otsuka H, Igase K, Yoshimura H, Sakanaka M (1996) Interleukin-6 prevents ischemia-induced learning disability and neuronal and synaptic loss in gerbils. Neurosci Lett 204:109–112. https://doi.org/10.1016/0304-3940(96)12340-5
47. Suzuki S, Tanaka K, Suzuki N (2009) Ambivalent aspects of interleukin-6 in cerebral ischemia: inflammatory versus neurotrophic aspects. J Cereb Blood Flow Metab 29:464–479. https://doi.org/10.1038/jcbfm.2008.141
48. Orzyłowska O, Oderfeld-Nowak B, Zaremba M, Januszewski S, Mossakowski M (1999) Prolonged and concomitant induction of astroglial immunoreactivity of interleukin-1β and interleukin-6 in the rat hippocampus after transient global ischemia. Neurosci Lett 263:72–76. https://doi.org/10.1016/S0304-3940(99)00043-9
49. Gertz K, Kronenberg G, Kälin RE, Baldinger T, Werner C, Balkaya M, Eom GD, Hellmann-Regen J et al (2012) Essential role of interleukin-6 in post-stroke angiogenesis. Brain 135:1964–1980. https://doi.org/10.1093/brain/aws075
50. Hsu M-P, Frausto R, Rose-John S, Campbell IL (2015) Analysis of IL-6/gp130 family receptor expression reveals that in contrast to astroglia, microglia lack the oncostatin M receptor and functional responses to oncostatin M: OSMR is in astroglia but not microglia. Glia 63:132–141. https://doi.org/10.1002/glia.22739
51. Gadient RA, Otten U (1996) Postnatal expression of interleukin-6 (IL-6) and IL-6 receptor (IL-6R) mRNAs in rat sympathetic and sensory ganglia. Brain Res 724:41–46. https://doi.org/10.1016/0006-8993(96)00264-8
52. Dziennis S, Jia T, Ronnekleiv OK, Hurn PD, Alkayed NJ (2007) Role of signal transducer and activator of transcription-3 in estradiol-mediated neuroprotection. J Neurosci 27:7268–7274. https://doi.org/10.1523/JNEUROSCI.1558-07.2007

53. Kinouchi T, Kitazato KT, Shimada K, Yagi K, Tada Y, Matsushita N, Sumiyoshi M, Satomi J et al (2012) Activation of signal transducer and activator of transcription-3 by a peroxisome proliferator-activated receptor gamma agonist contributes to neuroprotection in the peri-infarct region after ischemia in oophorectomized rats. Stroke 43:478–483. https://doi.org/10.1161/STROKEAHA.111.618926
54. Qin Z, Tao L, Chen X (2007) Dual roles of NF-κB in cell survival and implications of NF-κB inhibitors in neuroprotective therapy. Acta Pharmacol Sin 28:1859–1872. https://doi.org/10.1111/j.1745-7254.2007.00741.x
55. Giridharan S, Srinivasan M (2018) Mechanisms of NFκB p65 and strategies for therapeutic manipulation. J Inflamm Res 11:407–419. https://doi.org/10.2147/JIR.S140188
56. Sakurai H, Chiba H, Miyoshi H, Sugita T, Toriumi W (1999) IκB kinases phosphorylate NF-κB p65 subunit on serine 536 in the transactivation domain. J Biol Chem 274:30353–30356. https://doi.org/10.1074/jbc.274.43.30353
57. Sasaki CY, Barberi TJ, Ghosh P, Longo DL (2005) Phosphorylation of RelA/p65 on serine 536 defines an IκBα-independent NF-κB pathway. J Biol Chem 280:34538–34547. https://doi.org/10.1074/jbc.M504943200
58. O'Mahony AM, Montano M, Van Beneden K et al (2004) Human T-cell lymphotropic virus type 1 tax induction of biologically active NF-κB requires IκB kinase-1-mediated phosphorylation of RelA/p65. J Biol Chem 279:18137–18145. https://doi.org/10.1074/jbc.M401397200
59. Mandrekar P, Jeliazkova V, Catalano D, Szabo G (2007) Acute alcohol exposure exerts anti-inflammatory effects by inhibiting IκB kinase activity and p65 phosphorylation in human monocytes. J Immunol 178:7686–7693. https://doi.org/10.4049/jimmunol.178.12.7686
60. Zhang W, Potrovita I, Tarabin V, Herrmann O, Beer V, Weih F, Schneider A, Schwaninger M (2005) Neuronal activation of NF-κB contributes to cell death in cerebral ischemia. J Cereb Blood Flow Metab 25:30–40. https://doi.org/10.1038/sj.jcbfm.9600004
61. Clemens JA (2000) Cerebral ischemia: gene activation, neuronal injury, and the protective role of antioxidants. Free Radic Biol Med 28:1526–1531. https://doi.org/10.1016/S0891-5849(00)00258-6
62. Ridder DA, Schwaninger M (2009) NF-κB signaling in cerebral ischemia. Neuroscience 158:995–1006. https://doi.org/10.1016/j.neuroscience.2008.07.007
63. Zhou J, Li M, Jin W-F, Li XH, Zhang YY (2018) Role of NF-κB on neurons after cerebral ischemia reperfusion. Int J Pharmacol 14:451–459. https://doi.org/10.3923/ijp.2018.451.459
64. Bhakar AL, Tannis L-L, Zeindler C, Russo MP, Jobin C, Park DS, MacPherson S, Barker PA (2002) Constitutive nuclear factor-κ B activity is required for central neuron survival. J Neurosci 22:8466–8475
65. Song YS, Lee Y-S, Narasimhan P, Chan PH (2007) Reduced oxidative stress promotes NF-κB-mediated neuroprotective gene expression after transient focal cerebral ischemia: lymphocytotrophic cytokines and antiapoptotic factors. J Cereb Blood Flow Metab 27:764–775. https://doi.org/10.1038/sj.jcbfm.9600379
66. Yang J, Liao X, Agarwal MK, Barnes L, Auron PE, Stark GR (2007) Unphosphorylated STAT3 accumulates in response to IL-6 and activates transcription by binding to NFκB. Genes Dev 21:1396–1408. https://doi.org/10.1101/gad.1553707
67. Martincuks A, Andryka K, Küster A, Schmitz-van de Leur H, Komorowski M, Müller-Newen G (2017) Nuclear translocation of STAT3 and NF-κB are independent of each other but NF-κB supports expression and activation of STAT3. Cell Signal 32:36–47. https://doi.org/10.1016/j.cellsig.2017.01.006
68. Hwang CJ, Yun H-M, Jung YY, Lee DH, Yoon NY, Seo HO, Han JY, Oh KW et al (2015) Reducing effect of IL-32α in the development of stroke through blocking of NF-κB, but enhancement of STAT3 pathways. Mol Neurobiol 51:648–660. https://doi.org/10.1007/s12035-014-8739-0
69. Zhang L, Badgwell DB, Bevers JJ et al (2006) IL-6 signaling via the STAT3/SOCS3 pathway: functional analysis of the conserved STAT3 N-domain. Mol Cell Biochem 288:179–189. https://doi.org/10.1007/s11010-006-9137-3
70. Baker BJ, Akhtar LN, Benveniste EN (2009) SOCS1 and SOCS3 in the control of CNS immunity. Trends Immunol 30:392–400. https://doi.org/10.1016/j.it.2009.07.001
71. Raghavendra Rao VL, Bowen KK, Dhodda VK, Song G, Franklin JL, Gavva NR, Dempsey RJ (2002) Gene expression analysis of spontaneously hypertensive rat cerebral cortex following transient focal cerebral ischemia: GeneChip® analysis after stroke. J Neurochem 83:1072–1086. https://doi.org/10.1046/j.1471-4159.2002.01208.x
72. Wang X, Chen S, Ni J et al (2018) miRNA-3473b contributes to neuroinflammation following cerebral ischemia. Cell Death Dis 9:11. https://doi.org/10.1038/s41419-017-0014-7
73. Li T, Pang S, Yu Y, Wu X, Guo J, Zhang S (2013) Proliferation of parenchymal microglia is the main source of microgliosis after ischaemic stroke. Brain J Neurol 136:3578–3588. https://doi.org/10.1093/brain/awt287
74. Zhang S (2019) Microglial activation after ischaemic stroke. Stroke Vasc Neurol 4:71–74. https://doi.org/10.1136/svn-2018-000196
75. Sun M-S, Jin H, Sun X, Huang S, Zhang FL, Guo ZN, Yang Y (2018) Free radical damage in ischemia-reperfusion injury: an obstacle in acute ischemic stroke after revascularization therapy. Oxidative Med Cell Longev 2018:1–17. https://doi.org/10.1155/2018/3804979
76. Shirley R, Ord E, Work L (2014) Oxidative stress and the use of antioxidants in stroke. Antioxidants 3:472–501. https://doi.org/10.3390/antiox3030472
77. Chamorro Á, Dirnagl U, Urra X, Planas AM (2016) Neuroprotection in acute stroke: targeting excitotoxicity, oxidative and nitrosative stress, and inflammation. Lancet Neurol 15:869–881. https://doi.org/10.1016/S1474-4422(16)00114-9
78. Jung JE, Kim GS, Narasimhan P, Song YS, Chan PH (2009) Regulation of Mn-superoxide dismutase activity and neuroprotection by STAT3 in mice after cerebral ischemia. J Neurosci 29:7003–7014. https://doi.org/10.1523/JNEUROSCI.1110-09.2009
79. Ravindran S, Kurian GA (2019) Eventual analysis of global cerebral ischemia-reperfusion injury in rat brain: a paradigm of a shift in stress and its influence on cognitive functions. Cell Stress Chaperones 24:581–594. https://doi.org/10.1007/s12192-019-00990-4
80. Heo J, Han S, Lee S (2005) Free radicals as triggers of brain edema formation after stroke. Free Radic Biol Med 39:51–70. https://doi.org/10.1016/j.freeradbiomed.2005.03.035
81. Weis SM, Cheresh DA (2005) Pathophysiological consequences of VEGF-induced vascular permeability. Nature 437:497–504. https://doi.org/10.1038/nature03987
82. Geiseler S, Morland C (2018) The Janus face of VEGF in stroke. Int J Mol Sci 19:1362. https://doi.org/10.3390/ijms19051362
83. Dzietko M, Derugin N, Wendland MF, Vexler ZS, Ferriero DM (2013) Delayed VEGF treatment enhances angiogenesis and recovery after neonatal focal rodent stroke. Transl Stroke Res 4:189–200. https://doi.org/10.1007/s12975-012-0221-6
84. Yang J-P, Liu H-J, Liu X-F (2010) VEGF promotes angiogenesis and functional recovery in stroke rats. J Investig Surg 23:149–155. https://doi.org/10.3109/08941930903469482
85. Leng K, Xu Y, Kang P, Qin W, Cai H, Wang H, Ji D, Jiang X et al (2019) Akirin2 is modulated by miR-490-3p and facilitates angiogenesis in cholangiocarcinoma through the IL-6/STAT3/VEGFA signaling pathway. Cell Death Dis 10:262. https://doi.org/10.1038/s41419-019-1506-4

86. Shen Y, Gu J, Liu Z, Xu C, Qian S, Zhang X, Zhou B, Guan Q et al (2018) Inhibition of HIF-1α reduced blood brain barrier damage by regulating MMP-2 and VEGF during acute cerebral ischemia. Front Cell Neurosci 12:288. https://doi.org/10.3389/fncel.2018.00288
87. Zhang H-T, Zhang P, Gao Y, Li CL, Wang HJ, Chen LC, Feng Y, Li RY et al (2017) Early VEGF inhibition attenuates blood-brain barrier disruption in ischemic rat brains by regulating the expression of MMPs. Mol Med Rep 15:57–64. https://doi.org/10.3892/mmr.2016.5974
88. Valable S, Montaner J, Bellail A, Berezowski V, Brillault J, Cecchelli R, Divoux D, MacKenzie ET et al (2005) VEGF-induced BBB permeability is associated with an MMP-9 activity increase in cerebral ischemia: both effects decreased by ANG-1. J Cereb Blood Flow Metab 25:1491–1504. https://doi.org/10.1038/sj.jcbfm.9600148
89. Rosenberg GA, Estrada EY, Dencoff JE (1998) Matrix metalloproteinases and TIMPs are associated with blood-brain barrier opening after reperfusion in rat brain. Stroke 29:2189–2195. https://doi.org/10.1161/01.STR.29.10.2189
90. Tejima E, Guo S, Murata Y, Arai K, Lok J, van Leyen K, Rosell A, Wang X et al (2009) Neuroprotective effects of overexpressing tissue inhibitor of metalloproteinase TIMP-1. J Neurotrauma 26:1935–1941. https://doi.org/10.1089/neu.2009.0959
91. Fujimoto M, Takagi Y, Aoki T, Hayase M, Marumo T, Gomi M, Nishimura M, Kataoka H et al (2008) Tissue inhibitor of metalloproteinases protect blood-brain barrier disruption in focal cerebral ischemia. J Cereb Blood Flow Metab 28:1674–1685. https://doi.org/10.1038/jcbfm.2008.59
92. Li D-D, Song J-N, Huang H, Guo XY, An JY, Zhang M, Li Y, Sun P et al (2013) The roles of MMP-9/TIMP-1 in cerebral edema following experimental acute cerebral infarction in rats. Neurosci Lett 550:168–172. https://doi.org/10.1016/j.neulet.2013.06.034
93. Barr TL, Latour LL, Lee K-Y, Schaewe TJ, Luby M, Chang GS, el-Zammar Z, Alam S et al (2010) Blood-brain barrier disruption in humans is independently associated with increased matrix metalloproteinase-9. Stroke 41:e123–e128. https://doi.org/10.1161/STROKEAHA.109.570515
94. Amantea D, Tassorelli C, Russo R, Petrelli F, Morrone LA, Bagetta G, Corasaniti MT (2011) Neuroprotection by leptin in a rat model of permanent cerebral ischemia: effects on STAT3 phosphorylation in discrete cells of the brain. Cell Death Dis 2:e238. https://doi.org/10.1038/cddis.2011.125
95. Uzdensky AB (2019) Apoptosis regulation in the penumbra after ischemic stroke: expression of pro- and antiapoptotic proteins. Apoptosis 24:687–702. https://doi.org/10.1007/s10495-019-01556-6
96. Broughton BRS, Reutens DC, Sobey CG (2009) Apoptotic mechanisms after cerebral ischemia. Stroke 40:e331–e339. https://doi.org/10.1161/STROKEAHA.108.531632
97. Battle TE, Frank DA (2002) The role of STATs in apoptosis. Curr Mol Med 2:381–392. https://doi.org/10.2174/1566524023362456
98. Shyu W-C, Lin S-Z, Chiang M-F, Chen DC, Su CY, Wang HJ, Liu RS, Tsai CH et al (2008) Secretoneurin promotes neuroprotection and neuronal plasticity via the Jak2/Stat3 pathway in murine models of stroke. J Clin Invest 118:133–148. https://doi.org/10.1172/JCI32723
99. Suzuki S, Yamashita T, Tanaka K, Hattori H, Sawamoto K, Okano H, Suzuki N (2005) Activation of cytokine signaling through leukemia inhibitory factor receptor (LIFR)/gp130 attenuates ischemic brain injury in rats. J Cereb Blood Flow Metab 25:685–693. https://doi.org/10.1038/sj.jcbfm.9600061